Royleanones

Subjects: Chemistry, Medicinal | Pharmacology & Pharmacy
Contributor: Patrícia Rijo, Alfonso T. Garcia-Sosa

Plants have been used for centuries to treat several illnesses. The Plectranthus genus has a vast variety of species that has allowed the isolation of cytotoxic compounds with notable activities.
The abietane diterpenes 6,7-dehydroroyleanone (DeRoy), 7alfa-acetoxy-6-hydroxyroyleanone (Roy), and Parvifloron D (ParvD) were obtained from Plectranthus spp. and showed promising biological activities, such as cytotoxicity on several cancer cell lines, including cancer stem cell inducing sphere cells. In silico studies compared the possible binding modes of active compounds and derivatives against different PKC isoforms alpha/beta/delta/iota/lambda/theta/zeta.

Keywords: Plectranthus ; royleanones ; hemi-synthesis ; PKC activity ; isozyme-selectivity ; molecular interactions

1. MTT Breast Cancer

The inhibitory effects of the different natural royleanones (**1**-**3**) were compared in MFC-7, SkBr3, SUM159, and SUM159 grown in CSC-inducing conditions. CSC represents the subpopulation of cancer cells that is responsible for metastasis. Due to their morphological characteristics of growth in spheres, they are referred to as SUM159 spheres. Three-dimensional in vitro models can be considered as an intermediate model between in vitro cancer cell line cultures and in vivo tumor. Different cancer cell lines were used aiming to assess which of the cell development phases is most affected by the action of each abietane compound.

The results showed that increased concentrations of abietanes reduced cell viability (Figure 1). Overall, although Roy (**2**) and ParvD (**3**) tend to inhibit MCF-7, SkBr3, and SUM159 cell viability, it was shown to be less effective against the most aggressive type of cells, the cancer stem cells SUM159 sphere. DeRoy (**1**) showed the highest inhibitory effect on SUM159 spheres, thus indicating its potential to significantly decrease the number of viable CSC cells.

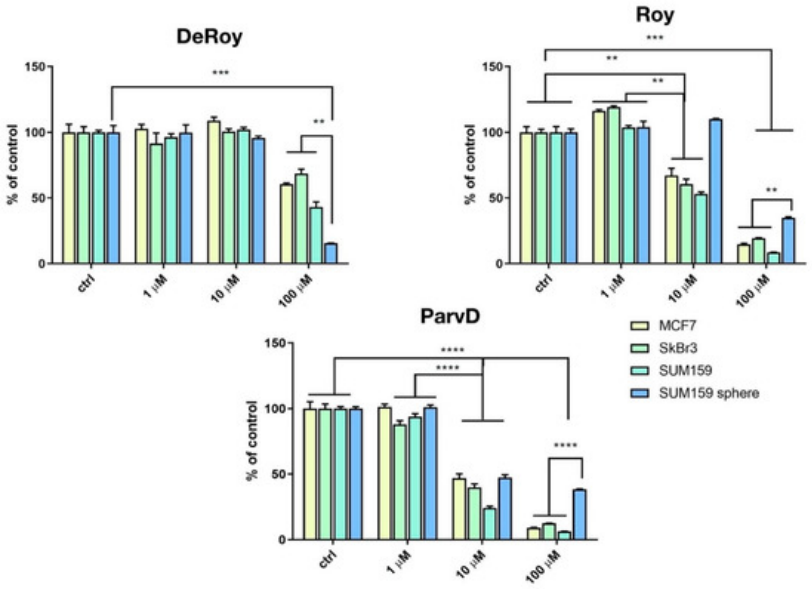

Figure 1. Cytotoxicity activity (MTT assay) on MCF-7 (hormone-positive breast cancer cells), SkBr3 Her-positive, SUM159 triple-negative, and SUM159 spheres. Statistical significance between marked groups: ** $p < 0.01$, *** $p < 0.001$, **** $p < 0.0001$.

2. Docking Results

The Protein DataBank (PDB, [1]) had the following available protein crystal structures: *θ*: 5F9E; *ι*: 3ZH8, 3AW8, 3A8X (only 3ZH8 has a co-crystallized inhibitor); *α*: 4RA4; and *β*II: 2I0E. There are crystal structures of other isomorphs; however, structures 1YRK and 2YUU (*δ*), and 2WH0 (*ε*) do not contain the catalytic domain, while no structure of the *ζ* isoform is available. From the percent identity matrix (Table 1), isomorph *θ* seems to be the most similar to isoform *δ*. Based on these results, we took structures 4RA4 for isoform *α*, 3ZH8 for isoform *ι* as an approximation to *ζ*, and 5F9E for isoform *θ* (and as an approximation to isoform *δ*). Isoform *α* was taken as an approximation to isoform *ε*. 1PTR was taken for isoform *δ*.

Table 1. Percent identity matrix from the sequence alignment of protein isoforms.

Uniprot, Isoform	*ζ*	*ι*	*δ*	*θ*	*ε*	*α*	*β*
sp|P41743|KPCI_HUMAN, *ζ*	100	72.81	36.82	36.86	44.78	43.57	43.48
sp|P41743|KPCI_HUMAN, *ι*	72.81	100	36.14	36.52	43.91	45.36	44.21
sp|Q05655|KPCD_HUMAN, *δ*	36.82	36.14	100	64.89	43.88	47.61	48.99
sp|Q04759|KPCT_HUMAN, *θ*	36.86	36.52	64.89	100	43.31	48.51	47.64
sp|Q02156|KPCE_HUMAN, *ε*	44.78	43.91	43.88	43.31	100	52.9	53.14
sp|P17252|KPCA_HUMAN, *α*	43.57	45.36	47.61	48.51	52.9	100	79.01
sp|P05771|KPCB_HUMAN, *β*	43.48	44.21	48.99	47.64	53.14	79.01	100

The results from the docking runs of all programs, proteins, and ligands (Table 2) showed that ParvD (**3**), Roy (**2**), and DeRoy (**1**) tended to have calculated docking scores close to those of the co-crystallized ligands (i.e., known binders) for all five isoforms studied. The MMGBSA results only showed a favorable calculated docking scores for **1** in isoforms *θ*, *β*, and *ι* but not in *α*. These results for the interaction can be compared to experimental observations showing that compounds **3** and **1** are the strongest inhibitors for all cell types. The weakest docking scores correspond to the compounds docked into the PKCδ isoform.

Table 2. Calculated docking scores for compounds against PKC isoforms. All values in kcal/mol.

Compound	5f9e (Isoform *θ*)			2i0e (Isoform *β*II)			3zh8 (Isoform *ι*)			4ra4 (Isoform α)			1ptr (Isoform *δ*)		
	Vina	Glide XP	MMGBSA	Vina	Glide XP	MMGBSA	Vina	Glide XP	MMGBSA	Vina	Glide XP	MMGBSA	Vina	Glide XP	MMGBSA
PMA	−7.4			−8.0	−4.84	−40.13	−7.2			−6.4			−4.7	−4.41	−42.12
ARA	−6.3			−7.8	−1.00	−40.95	−6.5			−5.6			−4.4	−1.85	−18.56
5VS1001 (5f9e co-cryst.)	−10.5	−7.2	−40.48												
PDS 902 (2i0e co-cryst.)				−11.0	−10.02	−56.23									
C581582 (3zh8 co-cryst.)							−9.9	−8.0	−58.56						
3KZ701 (4ra4 co-cryst.)										−10.4	−10.0	0			
PRB3 (1ptr co-cryst.)													−6.3	−4.25	−27.00
1 (DeRoy)	−9.3	−5.8	−44.29	−12.0	−6.21	−30.81	−8.4	−5.6	−36.23	−8.4	−6.7	0	−6.2	−4.13	−29.39
2 (Roy)	−9			−10.4			−8.8			−8			−6.7		
3 (ParvD)	−9.8	−2.0		−12.0	−5.84		−9.8	−6.91		−9.3	−4.84		−8.4	−4.68	
4 (RoyBz)	−9.3			−9.4			−9.0			−8.7			−6.9		

From the data presented in Table 1, Table 2, Table 3, Table 4, and Table 5, we can explain the general trends in the docking scores of royleanones to different isoforms of PKC. Docking calculations report docking scores of up to −9.9 kcal/mol for **1** and **3**. From the intermolecular interaction analysis (Table 3), **1** interacts with 11 amino acid residues in a hydrophobic manner. Kinases share overlapping substrate recognition patterns but specific hydrophobic binding pockets for recognizing bulky hydrophobic residues upstream of the catalytic Ser/Thr distinguish atypical PKCs from other kinases, and this may provide specificity. In addition, although reportedly forming a hydrophobic interaction with the conserved Lys 371, we cannot rule out the possibility for hydrogen bond formation as well, analogous to the case in the *α* isoform (with a corresponding conserved residue Lys 368). This actually is significantly different to compound **2**, as **1** is capable of forming this additional interaction. Moreover, a significant difference in the log*P* values (Table 5) between **2** and **1** makes the latter more favorable for the local hydrophilic environment of the binding site (Thr 404, Lys 371, Met 473, and Met 420, if considered as amphipathic), rather than the more lipophilic **2**. In addition, if we compare the percent of exposed surface area of the docked conformations in the PKC *α* isoform, **1** is more “buried”, and therefore more prone to keeping the bound conformation than **2**. Regarding **5** and **6**, both have similar binding patterns to compounds **2** and **1**. However, the Autodock docking score values are contradictory with respect to the experimental inhibition results. Therefore, the explanation may be found in the compounds’ properties. **5** has a similar log*P* value and ratio of the exposed surface as **1**, while **5** has the highest log*P* value and a more exposed surface. This is probably the reason for the lower interaction score: The compound is too nonpolar and less buried in the binding site, which contributes to an easier unbinding process. Figure 2 shows the difference in the exposed surface area for **1** and **5**.

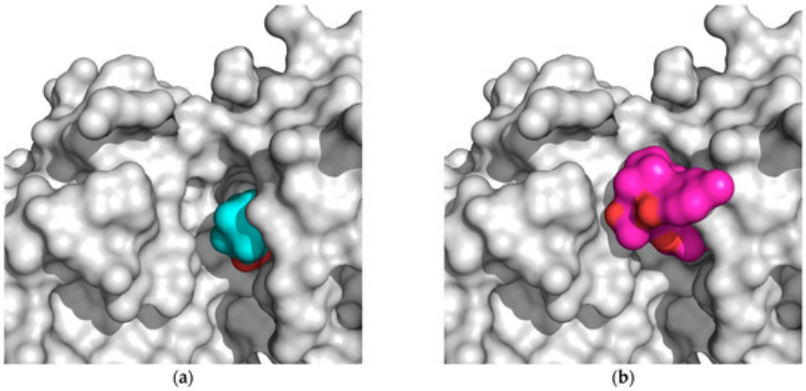

Figure 2. (**a**) Deeply bound and less exposed conformation of DeRoy (**1**, cyan) in PKC (white); (**b**) more exposed bound conformation of RoyBzCl (**5**, magenta) in PKC (white). All molecules in solvent-accessible surface area representation.

Table 3. PKC isoform binding site amino acids and corresponding interactions.

Compounds	PKC Isoform			
	α	***βI***	***ι***	***θ***
DeRoy (1)	**Met 417 (L), Ala 480 (L), Met 470 (L), Lys 368 (H), Val 353 (L), Leu 345 (L)**	**Met 473 (L), Ala 483 (L), Phe 485 (L), Leu 394 (L), Phe 353 (L), Val 356 (L), Lys 371 (L), Phe 418 (L), Met 420 (L), Ala 369 (L), Leu 348 (L)**	**Leu 376 (L), Thr 386 (R), Val 307 (L), Phe 297 (L), Ile 323 (L), Lys 274 (L), Val 259 (L), Ile 251 (L)**	**Leu 511 (L), Ala 521 (L), Met 458 (L), Lys 409 (H), Val 394 (H), Phe 391 (R)**
Roy (2)	**Val 420 (H), Lys 368 (L), Ala 366 (L), Met 417 (L), Val 353 (L), Leu 345 (H, L)**	**Met 473 (L), Ala 483 (L), Phe 353 (L), Met 420 (L), Lys 371 (L), Val 356 (L)**	**Asp 373 (H), Ile 323 (L)**	**Leu 511 (L), Asn 509 (L), Ala 521 (L), Met 458 (L), Lys 409 (L), Val 394 (L), Leu 386 (L)**
ParvD (3)	**Met 470 (L), Val 353 (L), Ala 366 (L), Leu 345 (L), Met 417 (R, L), Lys 368 (L), Leu 391 (L), Ala 480 (L)**	**Met 473 (L), Tyr 422 (L), Leu 348 (L), Val 356 (L), Ala 483 (L), Ala 369 (L), Asn 471 (H), Phe 485 (L), Leu 394 (L), Lys 371 (L)**	**Ile 251 (L), Val 259 (L), Leu 376 (L), Tyr 325 (H), Val 259 (L), Thr 386 (L), Lys 274 (L), Ile 323 (L), Val 307 (L), Phe 297 (L)**	**Leu 511 (L), Ala 521 (L), Met 458 (L), Ala 407 (L), Val 394 (L), Phe 391 (L)**
RoyBz (4)	**Asp 424 (H), Ala 366 (L), Val 353 (L), Met 417 (L), Lys 368 (L), Ala 480 (L)**	**Leu 348 (L), Met 473 (L), Val 356 (L), Phe 353 (L), Lys 371 (L), Met 420 (L), Ala 483 (L)**	**Phe 333 (L, R), Asp 330 (H), Ile 251 (L), Leu 376 (L), Val 259 (L), Thr 386 (R), Ala 272 (L), Ile 323 (L), Val 307 (L)**	**Gly 464 (L), Phe 391 (L), Val 394 (L), Ala 407 (L), Met 458 (L), Ala 521 (L), Asp 522 (L), Lys 409 (H)**

Compounds	PKC Isoform			
	α	*βI*	*ι*	*θ*
RoyBzCl (5)	Asp 424 (H), Gly 423 (L), Met 343 (R, L), Val 353 (L), Phe 350 (L), Lys 368 (L), Met 417 (L), Ala 480 (L)	Met 473 (L), Ala (483), Leu 394 (L), Met 420 (R, L), Lys 371 (L), Val 356 (L), Phe 353 (L), Leu 348 (L)	Phe 333 (R), Asp 330 (H), Thr 386 (R), Val 307 (L), Ile 323 (R), Ala 272 (R), Val 259 (R, L), Ile 251 (L), Arg 253 (R, L)	Leu 511 (L), Ala 521 (L), Lys 506 (L), Phe 391 (R), Val 394 (L), Leu 386 (R), Tyr 460 (L)
$RoyPr_2$ (6)	Asp 424 (H), Met 470 (L), Val 420 (L), Met 417 (L), Ala 366 (L), Val 353 (L)	Ala 483 (L), Phe 383 (L), Lys 371 (L), Val 356 (L), Leu 348 (L)	Thr 386 (H), Leu 376 (L), Ile 251 (L), Val 259 (L), Ala 257 (L)	Leu 511 (L), Ala 521 (L), Met 458 (L), Lys 409 (H, L), Ala 407 (L), Val 394 (L), Phe 391 (L)
DihydroxyRoy (7)	Met 470 (L), Val 420 (H), Met 417 (L), Lys 368 (L), Leu 345 (H, L)	Phe 353 (L), Leu 348 (L), Val 356 (L), Lys 371 (L), Met 420 (R, L), Leu 394 (L), Phe 485 (L), Ala 483 (L)	Asp 373, Val 259, Lys 274, Ala 272, Ile 323	Leu 511 (L), Ala 521 (L), Phe 523 (L), Leu 432 (L), Met 458 (L), Lys 409 (L), Val 394 (L), Leu 386 (L), Phe 391 (R)

Table 4. Corresponding amino acid residues in different PKC isoforms.

PKC*α*	PKC *β*I	PKC*ι*	PKC*θ*
Met 470	Met 473	Leu 376	Leu 511
Ala 480	Ala 483	Thr 386	Ala 521
Thr 401	Thr 404	Val 307	Thr 442
Met 417	Met 420	Ile 323	Met 458
Lys 368	Lys 371	Lys 274	Lys 409
Val 353	Val 356	Val 259	Val 394
Leu 345	Leu 348	Ile 251	Leu 386

Table 5. Compound octanol/water partition (log*P*) values and solvent-accessible surface area for docked poses in PKCα isoform.

Compound	Total Solvent Accessible Area ($Å^2$)	Solved Exposed Area in Docked Pose ($Å^2$)	Exposed Surface Ratio %	log*P*
DeRoy (1)	268.47	142.36	53.02	4.53
Roy (2)	318.47	209.29	65.71	2.65
ParvD (3)	171.75	355.37	48.12	5.64
RoyBz (4)	469.79	260.01	55.35	7.88
RoyBzCl (5)	504.92	323.30	64.03	8.8
$RoyPr_2$ (6)	403.77	207.97	51.50	4.87
DihidroxyRoy (7)	285.37	165.58	58.02	2.52

Compound **3** shows the best docking score towards the PKC *β*II isoform (−9.9 kcal/mol), however, without selectivity towards other isoforms. The high predicted affinity may be explained by the formation of more hydrophobic interactions with binding site amino acids than in the case of **1** and **2**. In addition, **3** has a higher log*P* value, and the ratio between the total solvent-exposed and docked conformation solvent-exposed surface is the lowest in the case of **3,** which indicates a slower unbinding process. Both properties are in favor of a higher predicted affinity towards any of the PKC isoforms.

The difference in docking scores between **1** and **4** can be explained by the scoring function's overestimation of hydrophobic interactions. The docking results identified **3** and **1** as the predicted most strongly interacting compounds to all PKC isoforms, although less strongly to *δ*. Finally, the predicted interaction of each compound in different PKC isoforms can be due to subtle but significant amino acid residue changes, such as Met → Leu or Thr → Val and others, which can change the electrostatic nature of the binding site towards being more hydrophobic.

The binding site of PKC*δ* can be seen to be aligned onto PKC*ι* (Figure 3). ParvD (**3**), DeRoy (**1**), and RoyBz (**4**) are moderately sized compounds compared to the others in this series, which may allow for a better fit in the different PKC binding sites, though PKC*δ* has a smaller binding site as compared to the other isoforms.

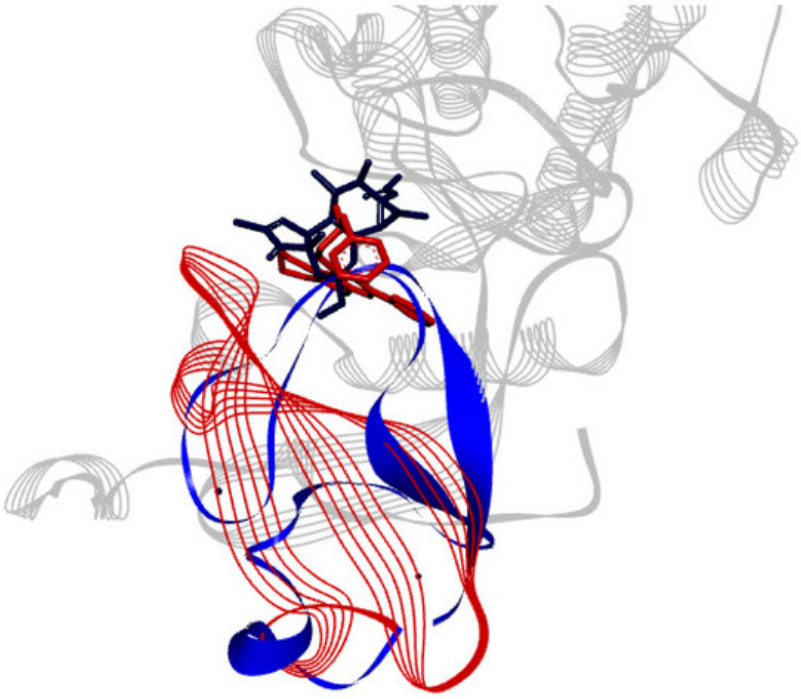

Figure 3. Alignment of tertiary structure of the catalytic binding sites for PKC*δ* (blue) and PKC*ι* (red).

ParvD (**3**) has the best interaction profile of **1**-**3**, given that it is the most potent compound against all cells studied, including the most aggressive type. The docked binding pose of ParvD (**3**) in 3ZH8 shows a significant difference with respect to DeRoy (**1**) (Figure 4), with the royleanone part of ParvD (3) flipped and more towards the entrance to the binding site, and its phenol ring in the hydroxybenzoate functional group interacting deeper, making hydrogen bonds with Val326 (top-right in Figure 4, interactions made instead by the royleanone part in the DeRoy(**1**) complex). Table 2 also shows that the strongest predicted interaction for the strongest experimental inhibitor, ParvD (**3**), is with isoform PKC*ι*, 3ZH8, where ParvD (**3**) outscores the other compounds, including DeRoy (**1**).

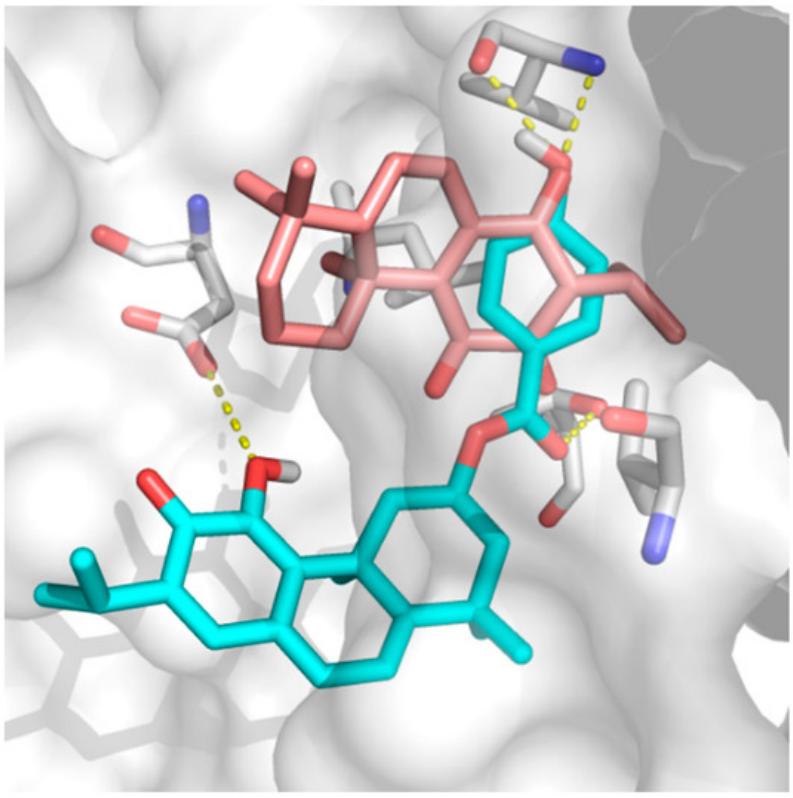

Figure 4. Docked binding poses of (**3**) ParvD (cyan) and (**1**) DeRoy (pink) in the binding site of PKC*ι*.

The 2-D interaction diagram (Figure 5) shows a schematic representation of the fit and intermolecular protein–ligand interactions for ParvD (**3**) and PKC*ι*.

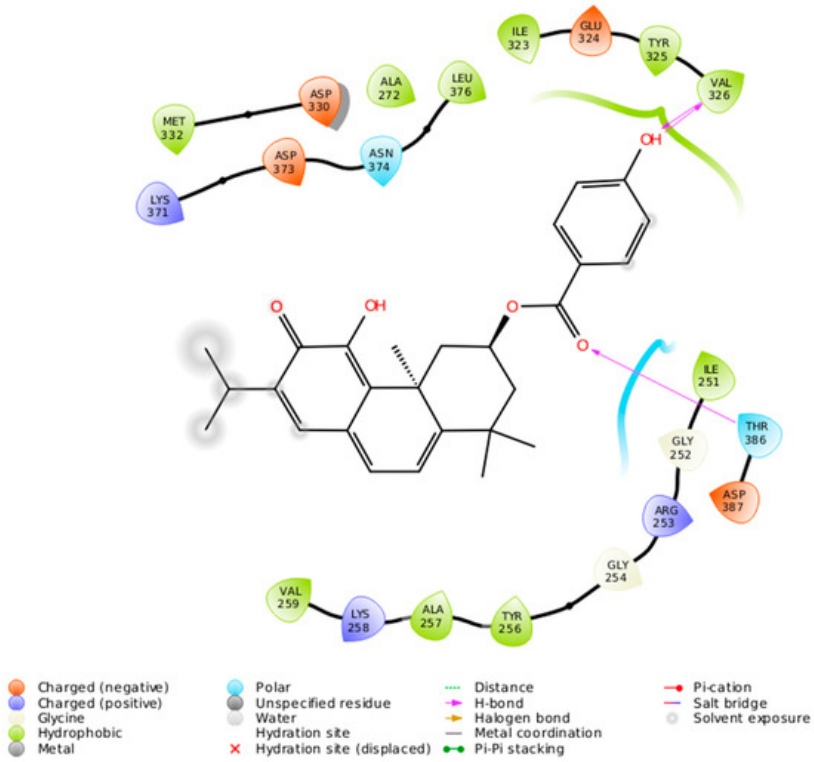

Figure 5. Intermolecular protein–ligand interactions for ParvD (**3**) in the binding site of PKC*ι*.

3. Discussion

Even though the mechanism of roylaneone compound inhibition of cancer cells is not yet determined as exclusively through inhibition or activation (**4** activates PKC*δ* [2]) of specific PKC isoforms, ParvD (**3**) has the best calculated interaction profile of compounds **1**-**3**, given its good interactions of the core structure and substituents with Val326 in the PKC binding site, as well as experimental inhibition against all cell types, including the most aggressive form. Structure 3ZH8, representing isoform PKC*ι*, appears to best reproduce experimental trends, and therefore, may provide clues for compound design. Substitution groups, such as hydroxybenzoate on position 4 of the royleanone core, can provide a better docked binding pose. In addition, polar groups at the mouth of the binding site are in close proximity to the 1,1 dimethyl groups. A possible route for further modification may be decorating or substituting these 1,1-methyl groups with polar functional groups able to make hydrogen bonds with these residues on PKC, such as –OH or $–NH_3$, as well as improving the compounds' log*P* value.

Clues on PKC isoform modulation may give information on the specificity towards each isoform based on the structure of their different biding sites, as well as on useful probe compounds, such as royleanones. Even if it may be difficult to pick up differences in the binding sites of PKC isoforms, this is indeed possible. Selective thieno[2,3-*d*]pyrimidine-based chemical inhibitors of atypical PKCs have been reported [3], and the region of hydrophobic residues in the binding site upstream from the catalytic Lys/Thr provides this specificity for compounds with bulky hydrophobic groups. The conserved Lys 371, on the other hand, provides a binding partner in nearly all isoforms. Atypical PKCs can tolerate the Lys -> Trp mutation, whereas other PKCs cannot [4].

Compounds in phase I or phase II clinical trials targeting classical PKC isoforms were not successful [5], but recent studies implicate that mainly atypical and novel PKC enzymes regulate oncogenic signaling pathways in pancreatic cancer. These subgroups converge signaling induced by mutant K-Ras, inflammatory cytokines, and growth factors. Approaches to compound design for novel PKCs and atypical PKCs may include allosteric inhibitors and ATP competitive inhibitors. The royleanone core and derivatives are interesting for further research on their different interactions with different PKC isoforms, pancreatic cancer, and breast cancer cell lines with an emphasis on breast CSC, which are attractive target cells as these are the cells with the highest metastatic potential.

References

1. Protein Data Bank. Research Collaboratory for Structural Bioinformatics. Available online: http://www.pdb.org/pdb/home/home.do (accessed on 16 December 2019).
2. Bessa, C.; Soares, J.; Raimundo, L.; Loureiro, J.B.; Gomes, C.; Reis, F.; Soares, M.L.; Santos, D.; Dureja, C.; Chaudhuri, S.R.; et al. Discovery of a Small-Molecule Protein Kinase Cδ-Selective Activator with Promising Application in Colon Cancer Therapy Article. Cell Death Dis. 2018, 9.
3. Svend Kjær; Mark Linch; Andrew Purkiss; Brenda Kostelecky; Phillip P. Knowles; Carine Rosse; Philippe Riou; Christelle Soudy; Sarah Kaye; Bhavisha Patel; et al. Adenosine-binding motif mimicry and cellular effects of a thieno[2,3-d]pyrimidine-based chemical inhibitor of atypical protein kinase C isoenzymes. *Biochemical Journal* **2013**, *451*, 329-342, 10.1042/bj20121871.
4. Susan F. Steinberg; Structural basis of protein kinase C isoform function.. *Physiological Reviews* **2008**, *88*, 1341-1378, 10.1152/physrev.00034.2007.
5. Peter Storz; Targeting protein kinase C subtypes in pancreatic cancer. *Expert Review of Anticancer Therapy* **2015**, *15*, 433-438, 10.1586/14737140.2015.1003810.
